MOLECULAR PHARMACOLOGY, 19:217-227

γ-Aminobutyric Acid Receptor Binding in Mammalian Brain

Heterogeneity of Binding Sites

RICHARD W. OLSEN, MARK O. BERGMAN, PAUL C. VAN NESS, SARAH C. LUMMIS, ANDREW E. WATKINS, CHRISTIAN NAPIAS, AND DONALD V. GREENLEE

Division of Biomedical Sciences and Department of Biochemistry, University of California, Riverside, California 92521

Received May 5, 1980; Accepted November 7, 1980

SUMMARY

OLSEN, R. W., M. O. BERGMAN, P. C. VAN NESS, S. C. LUMMIS, A. E. WATKINS, C. NAPIAS, AND D. V. GREENLEE. γ-Aminobutyric acid receptor binding in mammalian brain: heterogeneity of binding sites. *Mol. Pharmacol.* 19:217-227 (1981).

The binding of radioactive γ-aminobutyric acid (GABA) to receptor-like sites in mammalian brain membranes was analyzed by computer for comparison with models which might explain the observed apparent heterogeneity of ligand binding. The best fit was obtained with two independent binding sites. Binding was measured by centrifugation, using thoroughly washed, frozen, and thawed membranes without detergent treatment. Assays were carried out at 0° under sodium ion-free conditions which have previously been shown to allow detection only of those binding sites having the chemical specificity and other properties expected of receptor sites for the neurotransmitter GABA. Quantitative analysis of binding curves for several brain regions, subcellular fractions, and species revealed the general presence of two affinity classes for GABA receptors, one with K_D 0f 13 ± 6 nM (B_{max} = 0.33 pmole/mg of protein in bovine cortex) and the other with K_D of 300 ± 150 nM (B_{max} = 1.8 pmole/mg of protein in bovine cortex). The two-site model fit the data better than did models with one site, three sites, or negative cooperativity, but the fit to the mobile receptor-effector coupling hypothesis was almost as good as that of the two-site model. Consistent with the heterogeneity in equilibrium binding data, heterogeneity was also observed for association and dissociation rates of ligand binding and for rates of thermal inactivation of binding activity. The rate of heat denaturation was biphasic, with earlier times corresponding to selective loss of one of the two binding affinity subpopulations. Kinetics studies revealed two subpopulations of binding sites with respect to on- and off-rates. A slow component with $k_{+1} = 1.9 \times 10^7 M^{-1}$ min^{-1}, and $k_{-1} = 0.2$ min^{-1}, $K_D = 11$ nM, and low B_{max} corresponded to the high-affinity component of the equilibrium binding curve, and a rapidly dissociating population with lower affinity and higher B_{max} corresponded to the lower-affinity component of the equilibrium binding curve. Independent IC_{50} values for the high-affinity and low-GABA site were determined for a series of analogues. All analogues tested were more effective inhibitors of the high-affinity GABA sites, and a marked similarity in the relative drug potency for the two sites was observed. Thus the heterogeneity of GABA binding would appear to involve two discrete populations of receptors on the grounds of nonintercon-vertible heterogeneity under the conditions tested, whereas the similarity in the drug specificity of the two populations would be more consistent with a model involving multiple coupled or conformational states of a single receptor.

INTRODUCTION

GABA[1] meets many criteria for classification as the major inhibitory neurotransmitter in the CNS and has been implicated in numerous normal and abnormal aspects of brain function (1). One approach to the study of neurotransmitter function involves assay *in vitro* of postsynaptic receptor sites by suitable radioactive ligand binding. GABA synapses have been studied in this manner with binding assays employing radioactive GABA (2-11) or muscimol (12-14). Binding of GABA to well-washed membranes under Na^+-free conditions [to minimize association with nonreceptor uptake sites (2-4)] has

This work was supported by National Science Foundation Grant 77-24414, National Institutes of Health Grants NS-12422 and RR-09070, and by the Huntington's Chorea Foundation. Some of these results have appeared in abstract form [*Fed. Proc.* 39:1009 (1980)].

[1] The abbreviations used are: GABA, γ-aminobutyric acid; CNS, central nervous system.

0026-895X/81/020217-11$02.00/0

been demonstrated to meet many criteria of receptor specificity, including tissue localization and displacement by appropriate analogues (2–11, 15). The physiological response to GABA involves an increase in postsynaptic membrane permeability to chloride ions (16). This GABA receptor-chloride ion channel complex appears to be the site of action of various CNS excitatory drugs such as picrotoxin, which blocks GABAergic synapses (1, 4, 17–19), and depressant drugs, such as barbiturates and benzodiazepines, which enhance GABAergic transmission (19–21).

An important question that might be answered by radioactive ligand-binding studies is, how many distinct types of GABA receptors exist in the CNS? At this time the evidence is not clear whether more than one class of GABA receptors exists. The object of this study is to examine quantitatively the GABA receptor binding to brain membranes from a variety of mammalian species, brain regions, and subcellular fractions in order to determine whether apparent heterogeneity of GABA binding sites is a general property of the mammalian CNS, and whether this property represents distinct subtypes of GABA receptors.

MATERIALS AND METHODS

Membrane preparation. Mammalian brain membranes were prepared and assayed for GABA receptor binding as previously described (6, 22). Various brain regions from rat (freshly prepared) or from cow (frozen in 0.32 M sucrose for up to 6 months) were homogenized in 10 volumes of 0.32 M sucrose at 0° by eight passes of a motor-driven Teflon pestle (800 rpm) in a glass homogenizer tube (Thomas). The homogenate was centrifuged for 10 min at 2,000 rpm (1,000 × *g*) in Beckman rotor JA17 to yield a crude nuclear pellet which was discarded. The supernatant was centrifuged for 60 min at 150,000 × *g* (Beckman rotor 60 Ti, 45,000 rpm) to collect the crude mitochondrial, synaptosomal, and microsomal membranes, and the supernatant was discarded. In some cases separated synaptosomal or microsomal fractions were prepared by sucrose gradient centrifugation (6). Membrane fractions were twice disrupted with a tissuemizer (Ultra-Turrax, Tekmar Company, Cincinnati, Ohio) in 20 volumes of distilled water (osmotic shock) and centrifuged at 150,000 × *g* for 30 min. The resulting pellet was rehomogenized in buffer (0.05 M Tris adjusted to pH 7.1 with sodium-free citric acid) and frozen at −20°. These samples were thawed and centrifuged, and the pellets were homogenized, centrifuged, homogenized, and frozen again. On the day of assay the samples were thawed and centrifuged, the pellets were homogenized in the buffer to be used for assays, centrifuged once more, and homogenized for assay.

GABA receptor binding was measured by centrifugation (4–7) at 0–4° in Na^+-free buffer. [^{3}H]GABA (54–66 Ci/mmole; Amersham/Searle Corporation, Arlington Heights, Ill.) was included generally at 4 nM (approximately 175,000 cpm), with or without 0.1 mM nonradioactive GABA, to estimate nondisplaceable binding. Triplicate samples of approximately 1 mg of protein in an assay volume of 1 ml were incubated for 15 min at 0–4° followed by centrifugation (10 min at 50,000 × *g*, Beckman rotor JA20.1, 20,000 rpm). The supernatants were discarded and the pellets were twice rinsed superficially (without disruption) with 3 ml of cold buffer to remove unbound ligand from the sides of the tube. Rinsed pellets were solubilized overnight in 0.20 ml of Soluene-350 (Packard). Radioactivity was counted (Beckman LS-3155T) in 3 ml of toluene containing 0.5% (w/v) 2,5-diphenyloxazole (efficiency 33%). Protein was measured according to the method of Lowry *et al.* (23).

Data analysis. Binding data were analyzed by a nonlinear regression program, using an HP3000 computer. The essentials of the program are described as follows: the expression for ligand binding is given by

$$B = B_{\max} \cdot \frac{S}{K_D + S}$$

where B is the total amount of ligand bound at a free ligand concentration S, K_D is the dissociation equilibrium constant, and $B_{\max}$ is the total number of binding sites. Let us denote by B_i the experimental value for B at a ligand concentration of S_i. We further denote by σ_i the experimental error in B_i (σ_i is the standard deviation of replicate measurements of B_i). This procedure gives more weight to the more accurate data points. The difference between the experimental values and theoretical values as defined by the equation above can be described by

$$D = \sum_{i=1}^{n} \left(B_i - B_{\max} \cdot \frac{S_i}{K_D + S_i} \right)^2 \cdot \frac{1}{\sigma_i^2} \cdot \frac{1}{(n-2)}$$

where n is the number of data points (total number of ligand concentrations S_i at which binding B_i has been measured). D, in analogy to linear regression analysis, is a measure of the goodness of fit of the data to a given set of parameters K_D and $B_{\max}$. The computer will calculate these parameters for minimizing D.

Likewise, the expression for binding to two independent populations of binding sites is given by

$$B = B_{m1} \cdot \frac{S}{K_1 + S} + B_{m2} \cdot \frac{S}{K_2 + S}$$

where B_{m1} and B_{m2} are the $B_{\max}$ (number of sites) values for two sites having dissociation constants K_1 and K_2, respectively. Then

$$D = \sum_{i=1}^{n} \left(B_1 - \left[B_{m1} \cdot \frac{S_i}{K_1 + S_i} \right] - \left[B_{m2} \cdot \frac{S_i}{K_2 + S_i} \right] \right)^2 \cdot \frac{1}{\sigma_i^2} \cdot \frac{1}{(n-4)}$$

can be used to calculate the goodness of fit of the data to the equation for a given set of parameters K_1, K_2, B_{m1}, and B_{m2}. B_i is linear in B_{m1} and B_{m2}, and the computer program will calculate the values of B_{m1} and B_{m2} for various values of K_1 and K_2, using the data B_i, S_i, and σ_i. Likewise, similar equations have been applied for three independent populations of binding sites. The set of parameters which minimize D is the best fit of the data to these models.

The expression for binding with negative cooperativity is given by

$$B = \frac{S(K_2 + 2S) \cdot R_T}{K_1 \cdot K_2 + S(K_2 + S)}$$

where

$$R + S \leftrightharpoons RS, \quad \text{with} \quad K_1 = \frac{[R][S]}{[RS]} \quad \text{and}$$

$$RS + S \leftrightharpoons RS_2, \quad \text{with} \quad K_2 = \frac{[RS][S]}{[RS_2]}$$

and R_T is the total number of receptor sites. An analogous expression for three or four binding sites can be derived readily, and also the equations for calculating D values, the difference between the experimental data and the theoretical values defined by these equations. The computer then finds the values of K and R_T which minimize the D value.

Another model fit to the binding data was the mobile receptor-effector coupling model (24). In this model a single binding species (receptor, R) exists in multiple states which can bind ligand with different affinities (K_D) owing to the coupling of the receptor to other molecular complexes (E) which could be involved in carrying out the function of the receptor upon ligand binding, i.e., an effector, such as an ion channel or adenylate cyclase. This model differs from the multiple independent site example in that the different states of the receptor are in equilibrium, i.e., slowly interconvertible under the conditions of the assay. A limiting case of this model is the one in which no such interconversion occurs, in which case it is equivalent to the multiple independent sites model.

This model describes the following reactions involving the receptor (R), effector (E), and ligand (S):

$$\begin{aligned} R + S &\leftrightharpoons RS & K_1 &= [S][R]/[RS] \\ RS + E &\leftrightharpoons RSE & K_2 &= [RS][E]/[RSE] \\ R + E &\leftrightharpoons RE & K_3 &= [R][E]/[RE] \\ S + RE &\leftrightharpoons RSE & K_4 &= [S][RE]/[RSE] \end{aligned}$$

where K_1, K_2, K_3, and K_4 are the equilibrium dissociation constants for the reactions; they are related by $K_1 \cdot K_2 = K_3 \cdot K_4$. Note that K_1 and K_2 are ligand-binding reactions.

The parameters to be fit in this case are the equilibrium constants (three are independent), and the values for the total number of receptors R_T and the total number of effectors E_T. In a manner similar to that described above, one can compute values which will minimize D.

Since D is a function of the differences between the experimental data and the theoretical model, the smallest D value will result when the theoretical binding values (nonlinear regressions) show the smallest deviations from the experimental values for the various ligand concentrations; the deviations should fluctuate randomly in the positive and negative directions. The best fits (parameters giving minimal D value) for each model can then be compared with each other to determine the model with minimum D value (best fit model), and plotted for visual comparison with each other and with the experimental data.

RESULTS

The binding of [^{3}H]GABA as a function of free ligand concentration to cow cerebral cortex membranes at 0° is shown in Fig. 1. The membranes, consisting of a crude mitochondrial plus microsomal fraction, were prepared by the osmotic shock, multiple freeze-thaw, and buffer wash procedure which we have demonstrated to result in

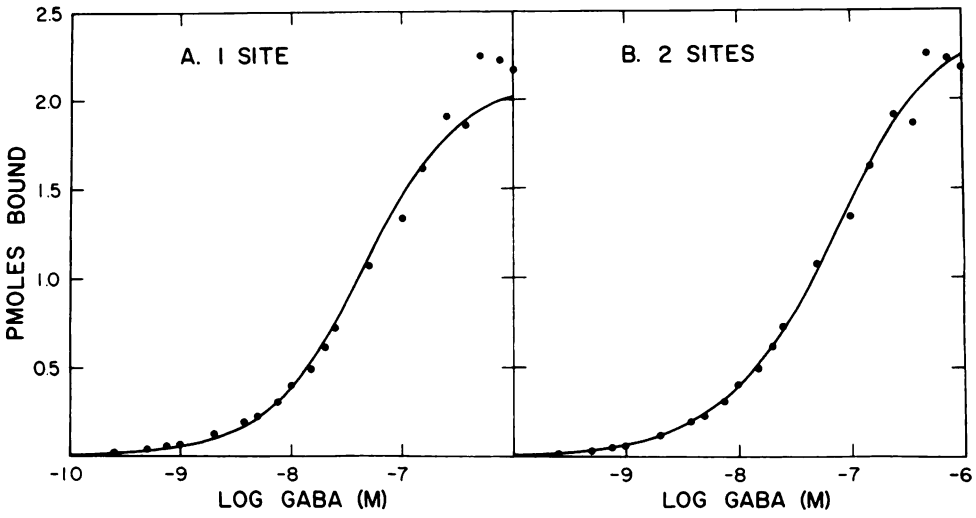

FIG. 1. *GABA receptor binding curve for bovine cortex: log concentration plot*

A. Binding data (●) with theoretical curve for one mass-action site (——) B. Same binding data with theoretical curve for two independent sites (——). Membrane preparation, binding assay, and data analysis are described under Materials and Methods. Results of this experiment, with 20 points in triplicate, are typical of numerous similar results (Table 1). Binding was measured by centrifugation, with protein at 1.0 mg/ml, in 50 mM Tris-citrate, pH 7.1, at 0°. Background was determined with 0.1 mM nonradioactive GABA. The concentration of [^{3}H]GABA, 66 Ci/mmole, was varied from 0.25–20 nM, and then a diluted stock solution of [^{3}H]GABA at 3.3 Ci/mmole was varied from 30 nM–3 μM. The signal to noise ratios at representative ligand concentrations were 300:130 cpm (0.25 nM), 8000:2000 cpm (10 nM), and 2000:8000 cpm (1 μM).

stable, reproducible binding and removal of endogenous tissue inhibitors of GABA binding (6, 22). GABA binding was measured under Na^+-free conditions by a centrifugation assay.

Figure 1A and B compares typically observed GABA receptor binding as a function of concentration data (●) with a computer-fitted theoretical curve (——) for either a single population of noncooperative binding sites (Fig. 1A) or with the equation for the summation of two independent classes of noncooperative and noninteracting sites (Fig. 1B). Under Materials and Methods, equations are described for various models of ligand binding for which computer programs were applied. The two-site model (Fig. 1B), in this and dozens of similar experiments, showed a better fit to the data than did the single-site model. A better fit of the data was also obtained for the two-site model than for a three-independent site model (not shown).

Further suggestion of apparent heterogeneity in GABA binding is provided by a Hill plot of the data, which yielded a slope of 0.86 ± 0.08 (mean ± standard error of the mean of four experiments). A Scatchard plot (Fig. 2A) of the data was curvilinear. The lower two straight lines depict the two individual binding curves whose sum produces the theoretical curve (*upper solid line*) in the two-site model, which shows an excellent fit with the data (●). The two binding sites thus described include a high-affinity site (K_{D1} = 7 nM, B_{m1} = 0.35 pmole/mg of protein) and a lower affinity site (K_{D2} = 100 nM, B_{m2} = 2.2 pmole/mg).

The binding data were also compared with a model for negative cooperativity and a model involving two interconvertible states of a mobile single receptor-effector coupling model (24), as is shown in the Scatchard plot of Fig. 2B. The two-site negative cooperativity model (Fig. 2B, ——) gave a much worse and the three-site negative cooperativity (- - -) a slightly worse fit than the independent two-site model.

The mobile receptor-effector model, (Fig. 2B, -·-·-) gave a reasonable fit to the data, but the best fits yielded equilibrium constants (see Materials and Methods) in which K_1 and $K_4 \gg K_2$ and K_3; that is, there was very little conversion between coupled and uncoupled states. Thus there is no advantage of this model over that with a fixed ratio of two independent populations. However, further information is needed to distinguish between these two models.

We have observed a similar heterogeneity of binding sites not only in bovine cortex, but also in several other regions of cow (19), rat (6), and human (25, 26) brain, prepared and assayed under these conditions. Computer analysis of sodium-independent GABA binding at 0° to well-washed membranes from all these tissues gave a best fit with the two-site model. Whereas B_{max} values varied considerably between brain areas as expected, the two apparent binding constants (K_D) were consistently in the range of 5–20 nM (K_{D1}) and 100–400 nM (K_{D2}). Table 1 includes these parameters for cow cortex (A), substantia nigra (F) and cerebellum (E), rat cortex (G), and human cortex (J). Likewise, neonatal rat brain binding (not shown) was similar to that of adult rat, and when rat cortex was fractionated by sucrose gradient centrifugation into separate synaptosomal (I) and microsomal (H) fractions, GABA binding was also best described by the two-site fit. The ratios of high- to low-affinity populations were similar but not identical in these various tissues; e.g., cerebellum had a slightly higher percentage of high-affinity sites than did cortex.

The variation in B_{max} and K_D values for a given tissue was considerable (Table 1, A) for different membrane

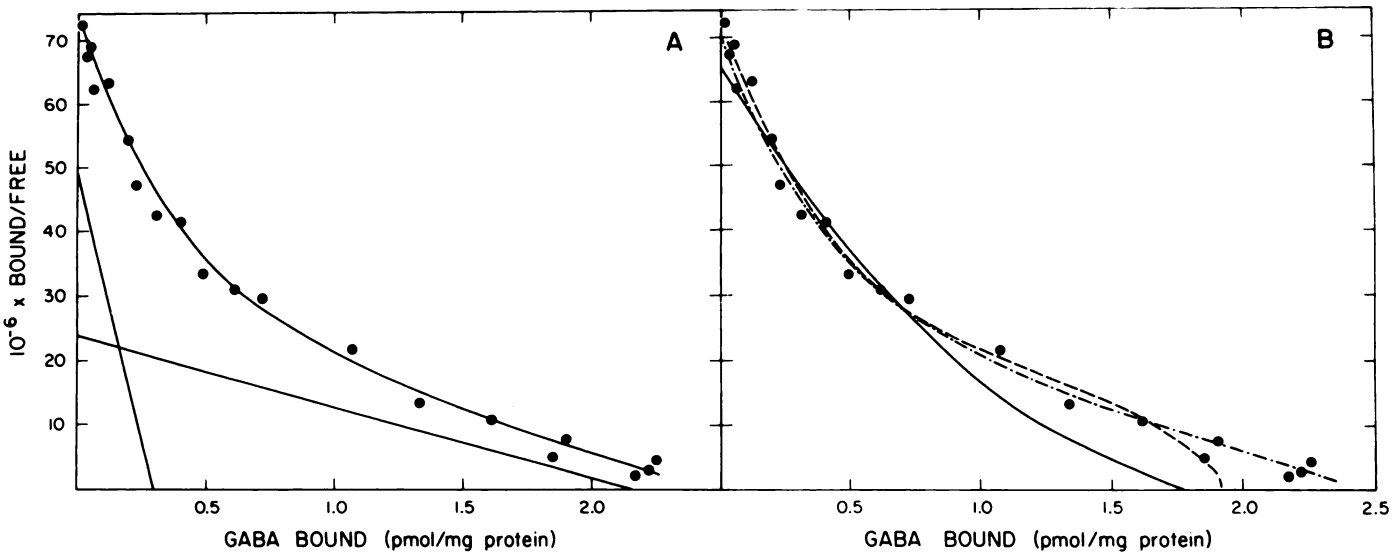

FIG. 2. *GABA receptor binding curve for bovine cortex: Scatchard plot.*

A. Same data as in Fig. 1. The *solid upper line* represents the theoretical curve for summation of the computer best-fit two-site model, with the two individual binding components represented by the *lower two lines*, including a higher-affinity component (K_D = 7 nM, B_{max} = 0.35 pmole/mg) and a lower-affinity component (K_D = 100 nM, B_{max} = 2.2 pmoles/mg).

B. Same data with computer fits for negative cooperativity (two sites, ——, or three sites, - - -) and for mobile receptor-effector coupling model (-·-·-) (see Materials and Methods). Each function plotted was the best fit for that model (minimal D value as defined in the text). The parameters for the receptor-effector coupling model were K_1 = 6 nM, K_2 = 0.46 nM, K_3 = 0.017 nM, K_4 = 150 nM, R_T = 2.53 pmoles/mg, and E_T = 2.35 pmoles/mg.

TABLE 1

GABA receptor binding in mammalian brain

Membranes were prepared as described under Materials and Methods, and consisted of well-washed, frozen, and thawed tissues, fraction $P_2 + P_3$, except where rat cortex was subfractionated by sucrose gradient centrifugation (6). Sodium-independent GABA binding was measured by centrifugation, as described under Materials and Methods, which also includes description of the computer data analysis. The binding parameters were derived from computer fits of binding curves involving triplicate measurements at 13–20 ligand concentrations, with the number of experiments (n) in parentheses. The GABA concentration was varied either by varying the amount of two stock solutions at 66 Ci/mmole and 3.3 Ci/mmole (Fig. 1), or by varying the concentration of undiluted [^{3}H]GABA from 0.25 nM to 4 nM, then varying the concentration of nonradioactive GABA at constant 4 nM [^{3}H]GABA. Background was determined with 0.1 mM nonradioactive GABA.

	Tissue	K_1	B_{m1}	K_2	B_{m2}
		nM	*pmoles/mg protein*	*nM*	*pmoles/mg protein*
A.	Bovine cortex (n = 26)	10.2 ± 8.5	0.33 ± 0.17	300 ± 160	1.77 ± 0.60
B.	Bovine cortex (n = 7)[a]	5.4 ± 3.9	0.36 ± 0.1	279 ± 151	1.63 ± 0.57
C.	Bovine cortex (n = 3)[b]	11.3 ± 1.5	0.57 ± 0.03	400 ± 0	2.66 ± 0.5
D.	Bovine cortex (n = 3)[c]	17 ± 0	0.30 ± 0.03	375 ± 25	1.72 ± 0.05
E.	Bovine cerebellum (n = 7)	13.6 ± 7.0	0.73 ± 0.12	371 ± 182	2.2 ± 0.8
F.	Bovine substantia nigra (n = 2)	6	0.04	400	0.35
G.	Rat cortex (n = 5)	25 ± 5	0.7 ± 0.3	212 ± 90	2.5 ± 0.9
H.	Rat cortex, microsomes (n = 4)	18 ± 5	0.25 ± 0.05	186 ± 122	1.63 ± 0.9
I.	Rat cortex, synaptosomes (n = 2)	9	0.22	286	3.2
J.	Human cortex (n = 13)	14 ± 5	0.35 ± 0.04	260 ± 50	1.45 ± 0.2

[a] A single membrane preparation was assayed seven times over a period of 4 weeks.

[b] One preparation was assayed on 3 consecutive days.

[c] One preparation was assayed three times on the same day.

preparations (perhaps related to efficiency of removal of endogenous inhibitors of binding (4, 6, 22, 26–28) as well as receptor protein stability), and for preparations with varying times of freezer storage. However, a given membrane preparation gave very reproducible binding curves over a period of at least several weeks, e.g., Table 1, B, C, and D.

The apparent heterogeneity of GABA binding sites in various mammalian brain species, regions, ages, and fractions is best fit by a model with two discrete binding sites, but other models might be applicable if an interconversion between different states could be observed under other assay conditions. Figure 3A shows the GABA binding activity as a function of pH, between 5.8 and 9.0, measured at one ligand concentration (4 nM). An optimum at pH 7.4–8.0 was observed, with almost twice as much binding at pH 7.5 as at pH 6.0 or 9.0. Figure 3B shows the variation of GABA binding with ionic strength, again measured at one GABA concentration (4 nM). This curve shows optimal binding at low ionic strengths (0.01–−0.1), with a plateau of somewhat lower activity at higher ionic strengths (0.1–0.3). Note that the "standard" assay conditions of 50 mM Tris-citrate, pH 7.1 (ionic strength = 0.09) are not optimal, neither with respect to pH nor to ionic strength.

GABA binding versus concentration was measured for cow cortex at pH 6.0 and in high salt (0.3 M KCl) for comparison to the curve obtained under the standard conditions. Whereas these extreme conditions could affect the binding affinities slightly, decreases in the levels of binding (B_{max} values) made it impossible to determine whether interconversion of populations was occurring. Binding curves measured at more optimal assay conditions (not shown) did not show significant variations in K_D or B_{max} as compared with the standard conditions. No significant interconversion of high- and low-affinity binding site subpopulations was observed for the few conditions tested thus far, but obviously all possible conditions have not been tried.

Heat denaturation studies can often determine whether more than one protein contributes to a given activity. Bovine cortex membranes were incubated for various times at 55°, then assayed at 0–4° for GABA binding. Figure 4 shows that the GABA binding activity was not lost with a single exponential decay rate, but with heterogeneous kinetics, reasonably well described by two rate processes. Approximately one-half of the binding activity seen under these assay conditions (10 nM [^{3}H]GABA, 0–4°, 50 mM Tris-citrate, pH 7.1) was lost at 55° with a half-life of approximately 7 min; the remainder was more stable, with a heat inactivation half-time of approximately 60 min.

Binding curves measured on samples pretreated at 55° for 20 min revealed a loss of binding sites without major changes in K_D. The ratio of high- to low-affinity sites did not remain the same, however. The low-affinity population (K_D = 100nM) was selectively more diminished by the heat treatment (B_{max} decreasing 76% from 2.2 to 0.5 pmole/mg) than was the high (K_D = 15 nM)-affinity population (B_{max} decreasing only 43% from 0.35 to 0.2 pmole/mg). In four experiments, binding curves performed on heat-treated membranes revealed a 75 ± 20% decrease in B_{max2} (low-affinity sites) and a 30 ± 15% decrease in B_{max1} (high-affinity sites). This is consistent with the differential heat sensitivity of the two populations implied by Fig. 4, with the low-affinity subpopulation apparently more easily denatured, and conversion of high affinity to low affinity not occurring. The biphasic curve for thermal inactivation rate is therefore consistent with the existence of two discrete noninterconvertible populations.

The apparent heterogeneity in equilibrium binding constants suggests that heterogeneity in association and dissociation rate kinetics for [^{3}H]GABA binding should

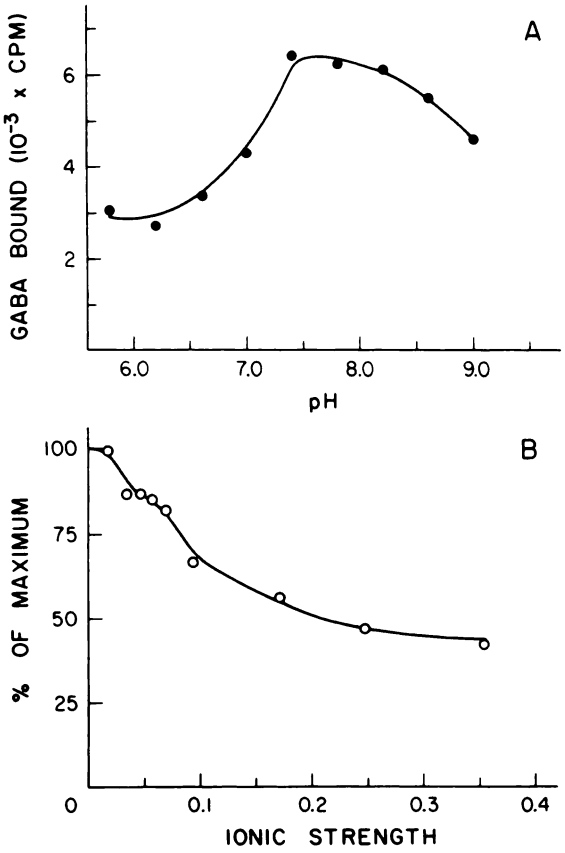

FIG. 3. *GABA receptor binding in bovine cortex at varying pH (A) and Ionic Strength (B)*

Membranes were prepared and assayed as described under Materials and Methods, with triplicate samples incubated with 4 nM [^{3}H]GABA (66 Ci/mmole) and background estimated with 0.1 mM nonradioactive GABA. The points represent the average of two experiments in each of two different buffer systems, in which the variation between the means was less than 10%.

A. Tris (50 mM) buffered at 0° to various pH values with sodium-free citric acid (ionic strength ≅ 0.09), or 50 mM KCl buffered to various pH values with 20 mM KH_2PO_4-K_2HPO_4 (ionic strength ≅ 0.10).

B. Tris-citrate at pH 7.1 was employed at different concentrations (0.01–0.1 M), or 20 mM KH_2PO_4-K_2HPO_4 (pH 7.1) was augmented with varying concentrations (0–0.3 M) of KCl. The 100% maximal binding was taken as the 10 mM Tris-citrate point.

also be present. Figure 5 demonstrates that this is indeed the case. The association rate for GABA binding could not be described by a single kinetic process (Fig. 5A). In 12 experiments, there was a slow component (minute time scale) of binding which did not extrapolate back to the origin; that is, there was a rapid component(s) of the binding reaction as well as a measurable slow component, indicating heterogeneous association kinetics.

Likewise, the dissociation of bound [^{3}H]GABA did not follow a single rate process (Fig. 5B). When excess (0.1 mM) nonradioactive GABA was added to membranes previously equilibrated for 30 min at 0–4° with [^{3}H]GABA (5–25 nM), approximately one-half of the bound GABA had dissociated within a few seconds, with a rate(s) too rapid to measure with the centrifugation assay. (Filtration assays were not suitable since washing the filters resulted in the loss of this rapidly dissociating component of the bound ligand.) The remaining portion of bound ligand dissociated with a much slower rate (half-life of 3.5 min, $k_{-1} = 0.20 \pm 0.02$ min^{-1}, mean ± standard error of the mean of 10 experiments).

The rapid (seconds or faster time scale) "on" rate(s) for GABA binding could not be determined accurately, but the rate constant for the slowly dissociating component could be measured. Two methods of estimating k_{+1} were applied, both utilizing the slope (k_{app}) of the logarithmic plot (Fig. 5A). Given the condition where the concentration of ligand greatly exceeds that of the receptor binding sites, then $k_{app} = k_{+1}[S] + k_{-1}$ (ref. 29). Since $k_{app} = 0.395$ min^{-1} (Fig. 5A), then $k_{+1} = 1.3 \times 10^7$ M^{-1}min^{-1} (assuming k_{-1} for the slow "on"-rate reaction to be that measured in Fig. 5B for the slow "off"-rate reaction, 0.2 min^{-1}). Then $K_D = k_{-1}/k_{+1} = 15$ nM, very close to the equilibrium dissociation constant for the high affinity component.

The second method (ref 30) of estimating k_{+1} uses the equation

$$k_{+1} = \frac{k_{app}}{S} \cdot \frac{B}{B_{max}}$$

By measuring k_{app} at three concentrations of [^{3}H]GABA, 5 nM, 15 nM, and 25 nM (three experiments each), we obtain average values of k_{app} for each ligand concentration. Assuming that the slow association involves the high-affinity component of the equilibrium binding curve, B and B_{max} values for the high-affinity subpopulation are employed to yield $k_{+1} = 2.5 \pm 0.8 \times 10$ M^{-1} min^{-1} (mean

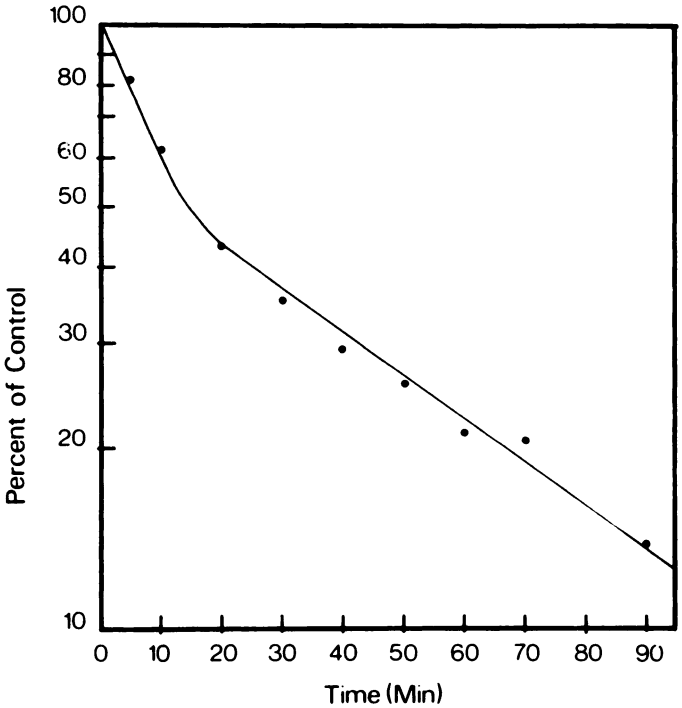

FIG. 4. *Thermal denaturation rate for GABA receptor binding*

Cortex membranes were prepared and assayed as described under Materials and Methods. Samples were pretreated at 55° for the times indicated, followed by equilibration to 0°, homogenization, and assay at 0° as usual. The points are the average of triplicates (variation 3%) and the experiment is typical of five.

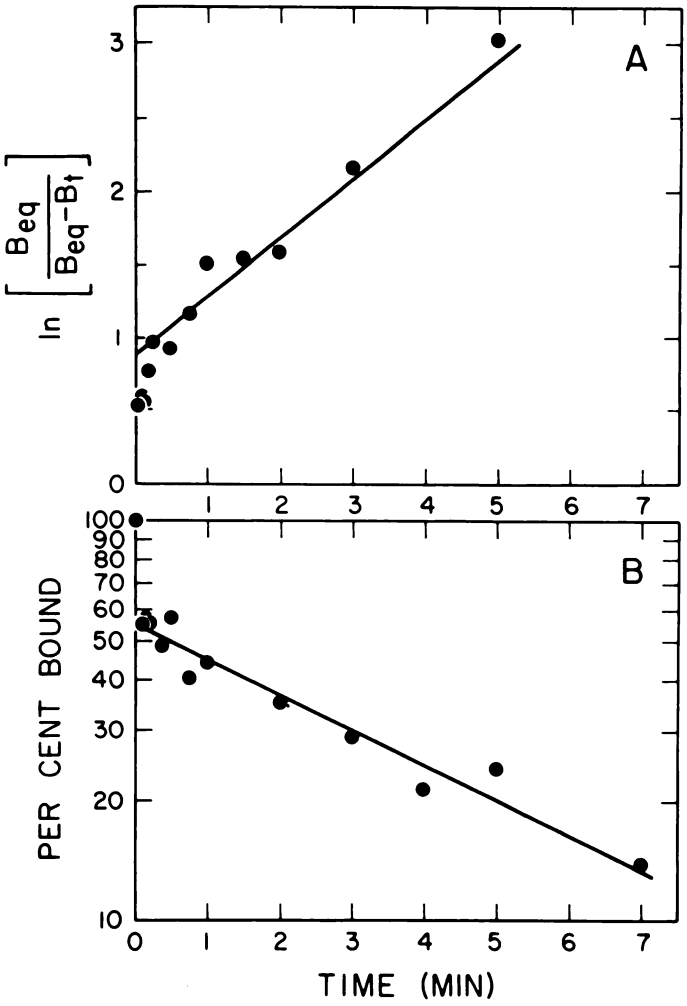

FIG. 5. *Kinetics of GABA receptor binding*

A. Association rate. Membranes were prepared as described above. Following incubation at 0° for the times indicated, membranes (1.0 mg/ml) in 50 mM Tris-citrate, pH 7.1, with 15 nM [^{3}H]GABA (66 Ci/mmole), were centrifuged for 3 min at 12,800 × *g* in Eppendorf microcentrifuge model 5412.

B. Dissociation rate. Following equilibration for at least 15 min at 0° with [^{3}H] GABA at 15 nM, samples were made 0.1 mM in nonradioactive GABA (10-μl aliquots in 1-ml assays) and centrifuged at the times indicated. Background was determined at equilibrium (>15 min) with 0.1 mM nonradioactive GABA. The bulk of the membranes was pelleted within a few seconds, so that the accuracy of time scale (*X* axis) was ± 15 sec. This variability, being the same for all points, would not alter the slope of the plot. Each point is the average of four experiments (variation <5%) and the plot is similar to that observed at other concentrations of GABA (see text). The pellets were superficially rinsed, solubilized, and counted as described under Materials and Methods. The binding parameters for the membrane preparation employed were K_1 = 7 nM, B_{m1} = 0.3 pmole/mg, K_2 = 200 nM, B_{m2} = 2.0 pmoles/mg, B_1 (15 nM) ≅ 0.3 pmole/mg, and B_2 (15 nM) ≅ 0.3 pmole/mg.

± standard error of the mean of nine experiments). Then $K_D = k_{-1}/k_{+1}$ = 8 nM for the slow component of GABA binding, again in agreement with the high-affinity equilibrium dissociation constant.

The ratio of the slow to fast component in kinetic experiments (*Y* intercepts in Fig. 5A and B) varied slightly with GABA concentration, giving a relatively greater percentage of rapidly associating and dissociating ligand at higher GABA concentrations and for tissue with a relatively higher ratio of low-affinity sites B_{m2}/B_{m1}, e.g., cortex > cerebellum (data not shown). This is consistent with the identification of high-affinity sites with the slow "on"- and "off"-rate populations.

This conclusion is further demonstrated by the following approach. By extrapolating the slow dissociation rate curve in experiments such as that shown in Fig. 5B back to zero time, one can estimate the fraction of total (equilibrium) moles of bound ligand associated with this slow off-rate population. One can approximate this measurement by adding excess nonradioactive GABA to equilibrated samples and centrifuging as rapidly as possible (within 10 sec), since there is a negligible perturbation of the equilibrium for this slow off-rate population, but virtually complete loss of the rapidly dissociating population. By varying the initial concentration of [^{3}H]GABA, the binding curve for the slow off-rate population of binding sites can be determined directly. The binding parameters of the fast off-rate subpopulation can be calculated by subtraction from the total binding (measured as usual at equilibrium). Figure 6 shows the Scatchard plots for a typical experiment measuring bovine cerebellum total binding (A) and slow off-rate sites (B). The equilibrium data gave the usual two-site fit, with K_{D1} = 13 nM (B_{max} = 0.7 pmole/mg) and K_{D2} = 350 nM (B_{max} = 2.1 pmole/mg). The slow off-rate binding gave a best fit of one site, K_D = 13 nM, B_{max} = 0.8 pmole/mg (Fig. 6B), in close agreement with the properties of the high-affinity site calculated from the equilibrium binding data. By subtraction of those data from the total binding (Fig. 6A), the computer analysis of the fast off-rate binding gave a best fit of one site with K_D = 200 nM, B_{max} = 2.4 pmoles/mg. In three experiments, the K_D value for the slowly dissociating subpopulation was 18 ± 10 nM (mean ± standard error of the mean); the B_{max} for this population was always 100 ± 25% of the B_{max1} value for the high-affinity population seen in equilibrium binding curves for the membrane preparation employed. Thus the kinetic hetergeneity indicates two populations of binding sites with properties showing excellent agreement with those described by the computer analyses of the equilibrium data, namely, a slower dissociating population with higher affinity and a faster dissociating population of lower affinity.

By using the centrifugation assay, we have previously measured (7, 19, 31) the IC_{50} values for inhibition of GABA receptor binding by numerous analogues. For example, the IC_{50} values for nonradioactive GABA and muscimol displacement of [^{3}H]GABA binding were 200 nM and 30 nM, respectively, measured with 20 nM [^{3}H]GABA, conditions under which a considerable fraction of labeled ligand would be bound to both high- and low-affinity subpopulations. With the technique described above for equilibrating samples with 2.5 nM [^{3}H]GABA, then adding 0.1 nM nonradioactive GABA and centrifuging immediately, the independent displacement of fast and slow off-rate sites by varying concentrations of GABA analogues could be determined. The IC_{50} values for all of the ligands were lower (higher affinity) for the slow off-rate sites than for the equilibrium binding (mixture of sites), e.g., 15 ± 2 and 5 ± 1 nM for GABA

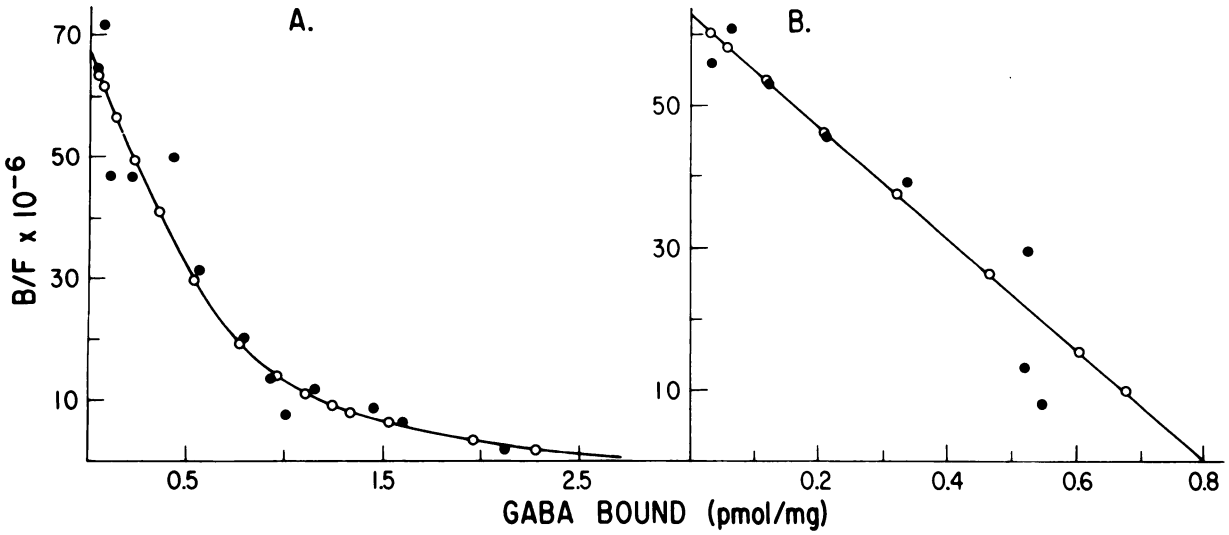

FIG. 6. *Scatchard plots of GABA receptor binding to cow cerebellum*

A. Total equilibrium. B. Slow off-rate binding only. Membranes were prepared and assayed as described under Materials and Methods. The data in B were obtained by adding 0.1 mM nonradioactive GABA to membranes previously equilibrated at 0° with various concentrations of [^{3}H]GABA and centrifuging immediately to give 10- to 15-sec time points. As is seen in Fig. 5B, the addition of excess nonradioactive GABA affects binding to the slowly dissociating component negligibly during the first 30 sec, and therefore this component can be considered to be still in equilibrium with the [^{3}H]GABA. By centrifuging the sample and quenching the reaction within 30 sec, the amount of ligand still bound at this point could be defined as slowly dissociating, and that fraction of the total was measured as a function of GABA concentration. ●, The data; ○, The computer fit (two-site model for A, one-site for B).

and muscimol under these conditions. Furthermore, all of the IC_{50} values for the slow off-rate sites were lower than those for the fast off-rate sites. A comparison of these independent IC_{50} values for 15 compounds gave a straight line (Fig. 7) (correlation, 0.965). The slope of this line was 1.02 ($p = 0.5$ as compared with a slope of 1.0), indicating that the same relative affinity was shown for these compounds to displace GABA from the rapidly dissociating populations as from the slowly dissociating subpopulations, with an average 5-fold higher concentration required for binding to the former (rapid, low-affinity) sites.

All of these data show that sodium-independent GABA receptor binding sites in mammalian brain involve more than one population (probably two). These two populations are not interconvertible under one set of thoroughly studied assay conditions, but may be related to each other by virtue of remarkably similar drug specificity.

DISCUSSION

GABA binding to brain homogenates might be expected to involve several classes of sites of which some, but certainly not all, classes may represent postsynaptic receptor sites. Other GABA binding proteins, including perhaps neuronal and glial transport recognition sites and enzymes, could contribute to such binding. In the absence of sodium ions, GABA binding to brain membranes, which have been thoroughly disrupted to destroy membrane integrity, does not appear to involve any association with the sodium ion-dependent uptake systems for GABA, and is restricted to a small quantity of high-affinity binding sites with receptor-like specificity (2–11, 15). One can also attempt (with some degree of success) to define specific receptor binding as that fraction of total GABA binding which is displaceable by pharmacological concentrations of receptor-specific GABA analogues, such as muscimol, 3-aminopropane sulfonic acid, or perhaps bicuculline, imidazole-acetic acid, or 1-aminocyclopentane-3-carboxylic acid (2, 4, 5, 7, 14, 15). Alternatively, one can attempt to measure specific receptor sites by using a receptor-specific radioactive ligand such as muscimol (12–14) or bicuculline (32).

However, even when studying receptor-specific binding with radioactive muscimol (12–14, 31), bicuculline (32), or the relatively well-characterized sodium-independent GABA binding (6, 10, 19, 22, 25, 26, 28, 33), more than one class of binding affinity has been observed under certain conditions of membrane preparation and assay. In particular, curvilinear slopes (apparent multiple-binding affinities) were seen for Scatchard plots of muscimol binding (12, 13, 31) and for GABA binding to Triton X-100-treated membranes (10, 28, 33). We observed that crude mitochondrial plus microsomal membranes from rat brain showed at least two binding affinities for GABA in well-washed membranes, even without detergent treatment (6, 19, 22, 25, 26, 31); observation of a very high-affinity binding site ($K_D \cong 15$ nM) was facilitated by using high specific radioactivity GABA and by thorough membrane washing to remove endogenous inhibitors of GABA binding present in the brain membranes (4, 6). These inhibitors, primarily tissue GABA itself (22, 26) but possibly including phospholipids (27) and/or protein (28) as well, probably account for some problems of reproducibility between different batches of membranes prepared from a given tissue.

In this study, we examined whether this observation of two or more classes of receptor-like GABA binding sites was consistently seen in brain membranes from numerous sources. The conclusion obtained is that two or more distinct classes of receptor-like GABA binding

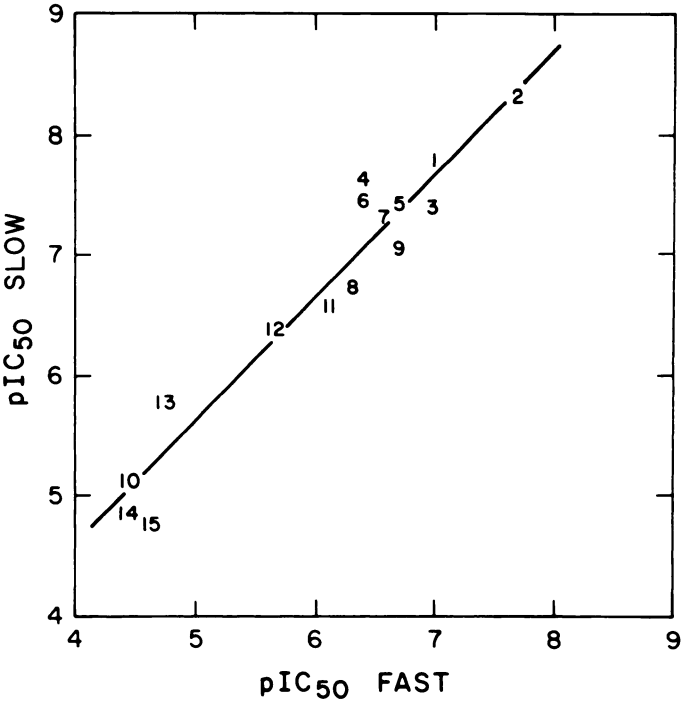

FIG. 7. *Comparison of independent GABA analogue affinities for high- and low-affinity receptor sites*

Membrane GABA binding was measured as described in legend for Fig. 6B by microcentrifugation, using 2.5 nM [^{3}H]GABA and 0.1 nM nonradioactive GABA for background. The extent of inhibition by various concentrations of analogues was measured in quadruplicate both at true equilibrium and 10–15 sec after the addition of 0.1 nM nonradioactive GABA, conditions under which the ligand bound to the rapidly dissociating subpopulation is essentially totally gone, and the ligand bound to the slowly dissociating subpopulation is essentially totally undisturbed (Fig. 5B). The extent of inhibition of the rapidly dissociating subpopulation was determined by subtracting the amount inhibited for the slowly dissociating sites from the amount inhibited for the total binding. IC_{50} values are an average of at least two determinations and are plotted as the negative log of the IC_{50} values (p IC_{50}). ——, Computer-derived linear regression. The compounds are as follows: *1*, GABA; *2*, muscimol; *3*, 3-amino-propane sulfonate; *4*, isoguvacine; *5*, piperidine-4-sulfonate; *6*, THIP (4,5,6,7-tetrahydroisoxazolo[5,4-c]pyridin-3-ol); *7*, (D)-β-hydroxy-GABA; *8*, (L)-β-hydroxy-GABA; *9*, *trans*-3-aminocyclopentane-1-carboxylate; *10*, *cis*-3-aminocyclopentane-1-carboxylate; *11*, imidazole acetate; *12*, bicuculline; *13*, β-alanine; *14*, taurine; *15*, benzyl penicillin. Compounds 2, 4, 5, and 6 were gifts of Dr. P. Krogsgaard-Larsen, Copenhagen, Denmark; compounds 3, 9, and 10 were gifts of Dr. G. A. R. Johnston, Sydney, Australia; and compounds 7 and 8 were gifts of Dr. D. Krause, Duarte, Calif.

sites are a general property of the mammalian CNS and that these sites are not interconverted *in vitro* under the conditions of assay and therefore could represent distinct entities. With the use of throughly washed membranes, computer analyses reveal two binding affinities as the best fit of sodium-independent GABA binding versus concentration curves for several species, ages, regions, and subcellular fractions of mammalian brain. Membranes from all of these sources consistently show one component of GABA binding with K_D = 13 ± 6 nM and a second component with K_D = 300 ± 150 nM. Less satisfactory computer fits were obtained for equations describing one or three sites or negative cooperativity, and no better fit was found for models involving two slowly interconvertible states of a single receptor. The two apparent populations of binding sites do not seem to be interconvertible under the assay conditions used, as shown not only by the equilibrium binding curves but also by heterogeneity in both the rates of thermal inactivation and in the binding kinetics. Both the association and dissociation rates were heterogeneous with a rapid component(s) difficult to measure and a slow component with $k_{+1} = 1.9 \times 10^7 M^{-1}$ min^{-1} and k_{-1} = 0.20 min^{-1} (K_D = 11 nM, average of nine experiments for bovine cortex). A similar K_D of 13 nM was measured for that fraction of the total GABA binding which had the slow dissociation rate. The binding of GABA to this slowly dissociating component could be measured independently of the faster binding sites by measuring the binding within 15 sec of the addition of excess nonradioactive GABA to previously equilibrated binding assays. During the first few seconds the radioactive ligand bound to rapidly dissociating sites is completely lost, whereas that bound to the slowly dissociating site is only negligibly dissociated and can be considered to be still at equilibrium. A similar method of characterizing high-affinity components of heterogeneous binding sites after first washing away the rapidly dissociating low-affinity components has been applied to kainic acid binding (34).

The same kinetic method was employed to measure the inhibition by GABA analogues of the high- and low-affinity GABA binding site populations independently. The slow off-rate population has the higher affinity for muscimol and several other GABA analogues. Interestingly, a marked correlation was seen in the potency of 15 compounds for inhibition of GABA binding to the high- and low-affinity subpopulations with an average 5-fold higher concentration needed for inhibition of rapidly dissociating, low-affinity sites.

The close similarity in relative chemical specificity suggests that the two populations might be closely related. This provides support for models explaining apparent heterogeneity of binding in terms of a single receptor existing in multiple states, such as coupled or uncoupled to effector systems (24, 35, 36). Such models are suggested for other receptor systems by evidence which includes (a) mass-action (homogeneous) binding curves for antagonist ligands combined with heterogeneous binding curves for agonist ligands; (b) perturbation of agonist binding curves by effectors such as guanine nucleotides, ions, or other unusual assay conditions; or (c) biochemical evidence for a single species of binding protein (24, 35, 36).

These three lines of evidence are much more scarce in the case of GABA receptors. For example, there are no antagonists available, with the possible exception of bicuculline, which also gives possibly heterogeneous binding (7, 10, 32). Differential effects of salts and detergents on GABA and bicuculline binding (10, 32), and nonlinear interactions between these two ligands (7, 19, 32), are most consistent with the presence of more than one class of sites. As yet no biochemical evidence for separation of multiple GABA binding proteins has been obtained. We obtained solubilized GABA receptor binding activity from bovine brain (31), which gave a binding curve for [^{3}H]muscimol with a best fit for one class of sites and

only one peak of activity on column chromatography. However, the yield of ≤50% membrane-binding activity solubilized left open the possibility of selective solubilization of one of two GABA binding components. A few experiments with varying assay conditions (ionic strength and pH) did not perturb the distribution of high- and low-affinity GABA binding sites. Futhermore, with the well-washed membranes in Tris-citrate buffer, pH 7.1, at 0–4°, we have not seen a perturbation of the binding curve by drugs such as picrotoxinin, barbiturates, or benzodiazepines, compounds known to affect postsynaptic GABA responses at sites distinct from, but coupled to, the GABA recognition sites (receptors) (17, 19, 21).

GABA and GABAergic agonists have been observed to enhance benzodiazepine binding to brain membranes *in vitro* (e.g., as reported in ref. 21). Although the concentrations of GABA agonists required for such an effect are higher than those required to inhibit sodium-independent GABA binding sites (either class) discussed in this paper, the rank order of activity is the same for GABA binding sites as for enhancement of benzodiazepine binding (or antagonism thereof) (21). Therefore, no unusual class of GABA receptor need be postulated to explain this action, although the difference in apparent binding affinities is unexplained. Another lower-affinity conformational state of the same receptor could be involved.

Neurophysiological evidence available does not prove, nor does it rule out, the possibility of multiple GABA receptors (37). These might be found on different cellular sites, such as synaptic and extrasynaptic membranes, or on synapses involved in presynaptic and postsynaptic GABAergic inhibition, or on distinct cell types. Our observation of only high-affinity sites on one line of cloned neuronal tumor cells (38) supports this hypothesis, but others have found both classes of GABA binding sites on a single cloned cell line (39).

If two or more distinct types of GABA binding sites existed, one might expect a variation in their ratio between different brain regions and fractions; we have observed a small variation. One might also expect differences, perhaps small, in the capacity of analogues to inhibit such GABA binding in different regions and fractions and under different assay conditions. Small regional variations in both ligand specificity (IC_{50} values) and in sensitivity to detergents have been seen in human brain (11). This would be consistent with variable ratios of high- to low-affinity GABA binding sites differing in other properties as well. Other studies supporting the idea of distinct receptors include unpublished observations of only one class of sites in discrete microdissections of brain,[2] only one class of sites in certain highly purified subcellular fractions,[3] or alterations in only one class of sites following lesions (40).

One could argue that the high-affinity site has too slow a dissociation rate ($t_{1/2}$ = 3.5 min) to match the observed rapid decay of the GABA-stimulated chloride conductance increase in the postsynaptic membrane, as determined by neurophysiological "noise" analysis in mammalian neurons (16). The low-affinity site might possess a rate sufficiently rapid to correspond to the millisecond responses to GABA (16). However, it is quite likely that homogenization and washing of membranes and/or the low temperature or low NaCl concentrations lead to changes in the properties of the receptor molecules. Measurement of binding kinetics under more physiological conditions ought to be more relevant to the question of the functional consequences of receptor ligand binding.

Interestingly, an excellent correlation has been found for the specificity of the GABA binding sites described here (both classes) and the lifetime of Cl^- channels on cultured mouse spinal cord neurons opened by receptors activated by GABA analogues (noise analysis) (41). However, much lower concentrations by orders of magnitude were needed for binding displacement than for biological activity; thus this correlation in chemical specificity might be considered as further evidence for multiple-affinity states of a single GABA receptor. Of course, there is also an excellent possibility of multiple classes of GABA receptors as well as multiple states for each class, but for the moment there appear to be two important classes of receptor-like [^{3}H]GABA binding sites.

[2] Candy, J. M., and I. L. Martin, First International Colloquium on Receptors: Neurotransmitters and Peptide Hormones, Capri, May 1979, Abstracts p. 123.

[3] Matus, A. I., and D. Wilkinson, First International Colloquium on Receptors: Neurotransmitters and Peptide Hormones, Capri, May 1979, Abstracts p. 101.

ACKNOWLEDGMENTS

We thank N. Birdsall, E. Hulme, B. Meiners, W. B. Levy, and D. Ching for helpful discussions, and A. Snowman for expert technical assistance.

REFERENCES

1. Roberts, E., T. N. Chase, and D. B. Tower, *GABA In Nervous System Function*. Raven Press, New York (1976).
2. Zukin, S. R., A. B. Young, and S. H. Snyder. Gamma-aminobutyric acid binding to receptor sites in rat central nervous system. *Proc. Natl. Acad. Sci. U. S. A.* **71**:4802–4807 (1974).
3. Enna, S. J., and S. H. Snyder. Properties of gamma-aminobutyric acid (GABA) receptor binding in rat brain synaptic membrane fractions. *Brain Res.* **100**:81–97 (1975).
4. Olsen, R. W., D. Greenlee, P. Van Ness, and M. K. Ticku. Studies on the gamma-aminobutyric acid receptor/ionophore proteins in mammalian brain, in *Amino Acids as Chemical Transmitters* (F. Fonnum, ed.). Plenum Press, New York, 467–486 (1978).
5. Olsen, R. W., M. K. Ticku, P. C. Van Ness, and D. Greenlee. Effects of drugs on γ-aminobutyric acid receptors, uptake, release and synthesis *in vitro*. *Brain Res.* **139**:277–294 (1978).
6. Greenlee, D. V., P. C. Van Ness, and R. W. Olsen. Endogenous inhibitor of GABA binding in mammalian brain. *Life Sci.* **22**:1653–1662 (1978).
7. Greenlee, D. V., P. C. Van Ness, and R. W. Olsen. Gamma-aminobutyric acid binding in mammalian brain: receptor-like specificity of sodium-independent sites. *J. Neurochem.* **31**:933–938 (1978).
8. Coyle, J. T., and S. J. Enna. Neurochemical aspects of the ontogenesis of GABAergic neurons in the rat brain. *Brain Res.* **111**:119–133 (1976).
9. Olsen, R. W., and K. Mikoshiba. Localization of gamma-aminobutyric acid receptor binding in the mammalian cerebellum: high levels in granule layer and depletion in agranular cerebella of mutant mice. *J. Neurochem.* **30**:1633–1636 (1978).
10. Enna, S. J., and S. H. Snyder. Influence of ions, enzymes and detergents on GABA receptor binding in synaptic membranes in rat brain. *Mol. Pharmacol.* **13**:442–453 (1977).
11. Enna, S. J., J. W. Ferkany, and P. Krogsgaard-Larsen. Pharmacological characteristics of GABA receptors in different brain regions, in *GABA-Neurotransmitters* (P. Krogsgaard-Larsen, J. Scheel-Kruger, and H. Kofod, eds.). Munksgaard, Copenhagen, 191–200 (1979).
12. Beaumont, K., W. Chilton, H. I. Yamamura, and S. J. Enna. Muscimol binding in rat brain: association with synaptic GABA receptors. *Brain Res.* **148**:153–162 (1978).
13. Wang, Y.-J., P. Salvaterra, and E. Roberts. Characterization of [^{3}H]muscimol binding to mouse brain membranes. *Biochem. Pharmacol.* **28**:1123–1128 (1979).
14. Meiners, B., P. Kehoe, D. M. Shaner, and R. W. Olsen. γ-Aminobutyric acid

receptor binding and uptake in membrane fractions of crayfish muscle. *J. Neurochem.* **32**:979–990 (1979).
15. Krogsgaard-Larsen, P., H. Hjeds, D. R. Curtis, D. Lodge, and G. A. R. Johnston. Dihydromuscimol, thiomuscimol, and related heterocyclic compounds as GABA analogues. *J. Neurochem.* **32**:1717–1724 (1979).
16. McBurney, R. M., and J. L. Barker. GABA-induced conductance fluctuations in cultured spinal neurons. *Nature* (*Lond.*) **274**:596–597 (1978).
17. Ticku, M. K., and R. W. Olsen. Picrotoxinin binding sites at the GABA synapse: a target for drug action. *Brain Res. Bull. Suppl. 2* **5**:213–216 (1980).
18. Ticku, M. K., M. Ban, and R. W. Olsen. Binding of [^{3}H]α-dihydropicrotoxinin, a γ-aminobutyric acid synaptic antagonist, to rat brain membranes. *Mol. Pharmacol.* **14**:391–402 (1978).
19. Olsen, R. W., M. K. Ticku, D. Greenlee, and P. Van Ness. GABA receptor and ionophore binding sites: interactions with various drugs, in *GABA-Neurotransmitters* (P. Krogsgaard-Larsen, J. Scheel-Kruger, and H. Kofod, eds.). Munksgaard, Copenhagen, 165–178 (1979).
20. Haefely, W., P. Polc, R. Schaffner, H. H. Keller, L. Pieri, and H. Möhler. Facilitation of GABAergic transmission by drugs, in *GABA-Neurotransmitters* (P. Krogsgaard-Larsen, J. Scheel-Kruger, and H. Kofod, eds.). Munksgaard, Copenhagen, 357–375 (1979).
21. Tallman, J. F., S. M. Paul, P. Skolnick, and D. W. Gallager. Receptors for the age of anxiety: pharmacology of the benzodiazepines. *Science* (*Wash. D. C.*) **207**:274–281 (1980).
22. Napias, C., M. O. Bergman, P. C. Van Ness, D. Greenlee, and R. W. Olsen. GABA binding in mammalian brain: inhibition by endogenous GABA. *Life Sci.* **27**:1001–1011 (1980).
23. Lowry, O. H., N. J. Rosebrough, A. L. Farr, and R. J. Randall. Protein measurement with the Folin phenol reagent. *J. Biol. Chem.* **193**:265–275 (1951).
24. Jacobs, S. and P. Cuatrecasas. The mobile receptor hypothesis and "cooperativity" of hormone binding. Application to insulin. *Biochim. Biophys. Acta* **443**:482–495 (1976).
25. Van Ness, P. C., and R. W. Olsen. Gamma-aminobutyric acid (GABA) receptor binding in human brain regions. *J. Neurochem.* **33**:593–596 (1979).
26. Olsen, R. W., P. C. Van Ness, C. Napias, M. Bergman, and W. W. Tourtellotte. Gamma-aminobutyric acid receptor binding and endogenous inhibitors in normal human brain and in Huntington's Chorea, in *Receptors for Neurotransmitters and Peptide Hormones* (G. Pepeu, M. J. Kuhar, and S. J. Enna, eds.). Raven Press, New York, 451–460 (1980).
27. Johnston, G. A. R., and S. M. E. Kennedy. GABA receptors and phospholipids, in *Amino Acids as Chemical Transmitters* (F. Fonnum, ed.). Plenum Press, New York, 507–516 (1978).
28. Toffano, G., A. Guidotti, and E. Costa. Purification of an endogenous protein inhibitor for the high affinity binding of gamma-aminobutyric acid to synaptic membranes of rat brain. *Proc. Natl. Acad. Sci. U. S. A.* **75**:4024–4028 (1978).
29. Bennett, J. P. Methods in binding studies, in *Neurotransmitter Receptor Binding* (H. I. Yamamura, S. J. Enna, and M. J. Kuhar, eds.). Raven Press, New York, 57–90 (1978).
30. Maelicke, A., B. W. Fulpius, R. P. Klett, and E. Reich. Acetylcholine receptor: responses to drug binding. *J. Biol. Chem.* **252**:4811–4830 (1977).
31. Greenlee, D. V., and R. W. Olsen. Solubilization of gamma-aminobutyric acid receptor protein from mammalian brain. *Biochem. Biophys. Res. Commun.* **88**:380–387 (1979).
32. Möhler, H., and T. Okada. Properties of γ-aminobutyric receptor binding with (+)-[^{3}H]bicuculline methiodide in rat cerebellum. *Mol. Pharmacol.* **14**:256–265 (1978).
33. Horng, J. S., and D. T. Wong. γ-Aminobutyric acid receptors in cerebellar membranes of rat brain after a treatment with Triton X-100 *J. Neurochem.* **32**:1379–1386 (1979).
34. London, E. D., and J. T. Coyle. Specific binding of [^{3}H]kainic acid to receptor sites in rat brain. *Mol. Pharmacol.* **15**:492–505 (1979).
35. Birdsall, N. J. M., C. P. Berrie, A. S. V. Burgen, and E. C. Hulme. Modulation of the binding properties of muscarinic receptors: evidence for receptor-effector coupling, in *Receptors for Neurotransmitters and Peptide Hormones* (G. C. Pepeu, M. J. Kuhar, and S. J. Enna, eds.). Raven Press, New York, 107–116 (1980).
36. Kent, R. S., A. DeLean, and R. J. Lefkowitz. A quantitative analysis of *beta*-adrenergic receptor interactions: resolution of high and low affinity states of the receptor by computer modeling of ligand binding data. *Mol. Pharmacol.* **17**:14–23 (1980).
37. Nistri, A., and A. Constanti. Pharmacological characterization of different types of GABA and glutamate receptors in vertebrates and invertebrates. *Prog. Neurobiol.* (*Oxf.*) **13**:117–235 (1979).
38. Napias, C., R. W. Olsen, and D. Schubert. GABA and picrotoxinin receptors in clonal nerve cells. *Nature* (*Lond.*) **283**:298–299 (1980).
39. Baraldi, M., A. Guidotti, J. P. Schwartz, and E. Costa. GABA receptors in clonal cell lines: a model for study of benzodiazepine action at the molecular level. *Science* (*Wash. D. C.*) **205**:821–823 (1979).
40. Guidotti, A., K. Gale, A. Suria, and G. Toffano. Biochemical evidence for two classes of GABA receptors in rat brain. *Brain Res.* **172**:566–571 (1979).
41. Barker, J. L., and D. A. Mathers. GABA analogues: high correlation between channel duration on cultured mouse spinal neurons and I/IC_{50} values at low affinity GABA receptor sites on frozen rat brain synaptic membranes. *Abstr. Soc. Neursci.* **6**:189 (1980).

Send reprint requests to: Dr. Richard W. Olsen, Division of Biomedical Sciences, University of California, Riverside, Calif. 92521.